THERMAL/HYDRAULIC BEHAVIOR OF MIXED-OXIDE FUEL PREPARED WITH WEAPONS-DERIVED PLUTONIUM[*] [†]

Larry J. Ott
Oak Ridge National Laboratory
P.O. Box 2008
Oak Ridge, Tennessee 37831-8057

Frederick P. Griffin
Oak Ridge National Laboratory
P.O. Box 2008
Oak Ridge, Tennessee 37831-8057

ABSTRACT

The Oak Ridge National Laboratory is currently managing a test irradiation of mixed-oxide (MOX) fuel for the U.S. Department of Energy Fissile Materials Disposition Program. This paper describes the thermal/hydraulic behavior of MOX fuel (prepared with weapons-derived plutonium) and the experimental components (clad and stainless steel containment) during the ongoing irradiation in the Advanced Test Reactor at the Idaho National Engineering and Environmental Laboratory.

An experiment-specific code has been developed at ORNL to model the double-containment configuration of the MOX test capsules. This code has been extensively applied in the preparation of the safety analyses that are required prior to irradiation and in pre- and postirradiation examination (PIE) MOX fuel pin performance calculations. It has been found, given the appropriate fuel densification parameters (derived from the PIE results), that available fuel models (employed in the experiment specific code and FRAPCON-3), which replicate the fuel behavior represented by the U.S. and European data, adequately describe the performance of the weapons-derived MOX.

Code-predicted fission gas release from the test MOX fuel has been in accordance with the European MOX literature, and the PIE gas release data fall slightly below the European trend for similar fuel heating rates. Clad creep and ridging observed in PIE profilometry of withdrawn test fuel pins has been shown to be caused by fuel pellet hourglassing during normal operation at high linear heat generation rates.

Fuel performance, to date, has been excellent and is consistent with code predictions and with U.S. and European experience.

INTRODUCTION

Mixed uranium-plutonium oxide (MOX) fuel utilization is supported by a large body of fuel irradiation experience, generated primarily in Europe. Most of this experience has been gained with reactor-grade plutonium, derived from reprocessed low-enriched uranium (LEU) fuel. An experiment containing weapons-derived MOX fuel is being irradiated in the Advanced

* The submitted manuscript has been authored by a contractor of the U.S. Government under contract No. DE-AC05-00OR22725. Accordingly, the U.S. Government retains a nonexclusive, royalty-free license to publish or reproduce the published form of this contribution, or allow others to do so, for U.S. Government purposes.

† Research sponsored by the Office of Fissile Materials Disposition, U.S. Department of Energy, National Nuclear Security Agency, under contract DE-AC05-00OR22725 with UT-Battelle, LLC.

Test Reactor (ATR) at the Idaho National Engineering and Environmental Laboratory (INEEL); an overview of this experiment is presented in the first paper of this session (Reference 1). The Oak Ridge National Laboratory (ORNL) manages this project for the Department of Energy.

This paper presents the thermal/hydraulic behavior of the mixed-oxide fuel (prepared with weapons-derived plutonium) and the experimental components during the ongoing irradiation in the ATR.

TEST CAPSULE MODELLING

As shown in the companion paper (Reference 1), each of the Zircaloy-clad MOX fuel pins is encapsulated in a stainless steel capsule containment. For drop-in experiments in the beryllium reflector of the ATR, the outer stainless steel shell fulfills a requirement of the ATR Technical Specifications that the experiment containment meet the intent of ASME B&PV Code Section III, Class 1, standards. No available fuels-modeling code is applicable for this double-containment configuration. In order to predict the response of the capsule assemblies in the MOX irradiation experiment, including the effects of fission gas release and fuel swelling during irradiation, ORNL developed the experiment-specific Capsule Assembly Response (Thermal and Swelling) [CARTS] code.

In essence, CARTS determines the one-dimensional coupled thermal/mechanical solution for the capsule assembly at the fuel pellet midplane for each time step in the advancement of the fuel burnup. In addition to thermal expansion of capsule components, the MOX fuel also undergoes dimensional changes due to irradiation. Initially, there is fuel densification such that the pellet-to-clad gap increases. Subsequently, with increased burnup, the fuel begins to swell (due to formation of gaseous and solid fission products) so that the gaps begin to shrink. CARTS employs state-of-the-art models (industry and NRC) for the fuel and gas gap behavior. The primary objectives of the CARTS code are to determine the radial temperature distribution within the capsule assembly, the extent of the gas gap closures, the strains in the Zircaloy and stainless steel walls as functions of the fuel pin pressurization, the component thermal expansions, and the fuel swelling and densification.

As shown in Figure 1, the CARTS-predicted operating envelope [linear heat generation rates (LHGRs) and fuel temperatures] for the MOX irradiation experiment is prototypic of commercial light water reactors (LWRs) with fuel of similar dimensions (the LWR envelope is determined at the peak axial location for the average core position, Reference 2). In general,

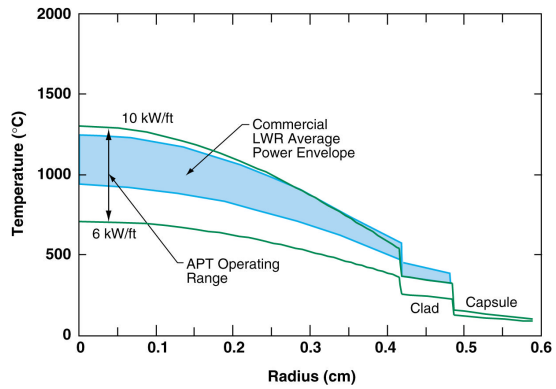

Fig. 1. Operating conditions (LHGRs and fuel/clad temperatures) for the MOX irradiation experiment are prototypic of commercial LWR fuel.

the average LHGR operating range for commercial PWRs is 5-7 kW/ft. The expected average LHGR for the MOX mission fuel will be less than 6 kW/ft. The as-run LHGRs for the test MOX capsules withdrawn at a burnup of 30 GWd/MT averaged 8.0 kW/ft during the first irradiation phase, 8.2 kW/ft in the second phase, and 5.5 kW/ft in the final phase prior to withdrawal. These test capsules have been conservatively operated at higher LHGRs and with more thermal cycles than the mission fuel will encounter.

In addition to the pre- and postirradiation examination (PIE) MOX fuel pin analyses, CARTS has also been extensively applied in the preparation of the safety analyses that are required prior to ATR irradiation. With respect to the fuel behavior, the primary safety concerns are fuel melting and excessive fuel swelling (that

might mechanically impact the clad to the extent that deformation of the stainless steel containment would affect the thermal/hydraulic response within the experiment assembly).

The initial safety analysis conservatively assumed a constant LHGR of 12 kW/ft (the maximum heating rate for these test capsules has been about 10.7 kW/ft), for which the maximum predicted fuel temperature remains more than 1000°C below the fuel melting temperature. Thus, fuel melting has not been a safety concern. However, these capsules were constructed with diametral gas gaps of 2-3.5 mils whereas commercial fuel pins have initial diametral gaps of 6.5-8.5 mils (Ref. 2); thus, for these test capsules, the primary safety concern is excessive fuel swelling.

CARTS employs industry- and NRC- sponsored fuel densification and swelling models (based on the available LEU and MOX experimental data base). Postirradiation examinations (PIEs) of withdrawn MOX capsule assemblies (described in a companion paper, Reference 3) provide evidence for assessing the behavior of the weapons-derived plutonium MOX fuel in this experiment.

For an assessment of the MOX test fuel performance, comparison of the clad and pellet dimensions as determined for successively higher burnups establishes the history of pellet swelling and clad creep as experienced at the pellet midplanes during irradiation. For each of the three withdrawals (at 9, 21, and 30 GWd/MT burnups, Ref. 3), the capsule and fuel pin metrological results were combined with measurements made directly from photographic enlargements of the metallographic mounts. This permitted determination of the clad thickness and internal diameter, the pellet outer diameter, and the effective gap between the pellet and the clad, which includes all internal pellet cracks as part of the gap. CARTS was then employed to facilitate interpretation of the PIE observations.

As shown in Figure 2, CARTS code predictions sufficiently reproduce the densification and swelling history (to 30 GWd/MT) for this fuel. Given the clad thermal boundary conditions from the CARTS analyses, the FRAPCON-3 fuels code (Reference 4) was executed for these capsule irradiation histories and the results are overlaid on the CARTS results in Figure 2. Given the appropriate fuel densification parameters (derived from the PIE results), these fuel models (which replicate the fuel behavior represented by the U.S. and European data) adequately describe the irradiated weapons-derived MOX fuel.

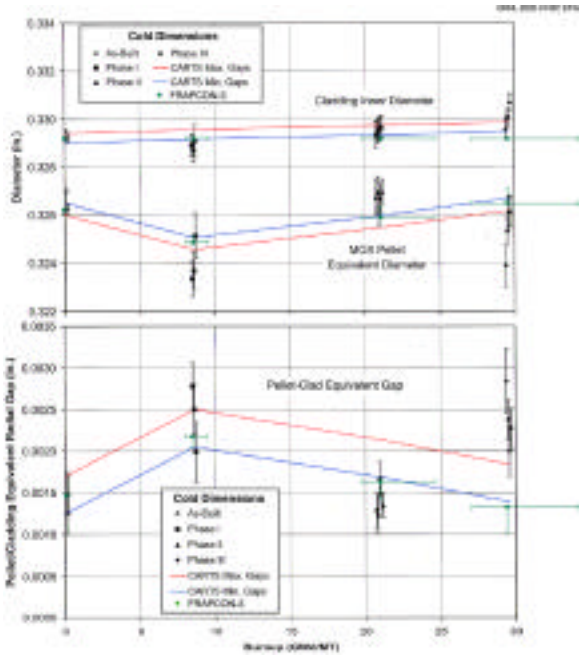

Fig. 2. PIE clad and pellet dimensional analyses with code predictions.

TEST CAPSULE BEHAVIOR DURING IRRADIATION

The 40 GWd/MT PIE now being performed at ORNL addresses Capsules 4 and 13, which occupied various symmetric test assembly positions during irradiation Phases I, II, III, and IV, accumulating a total of 904 EFPDs. The irradiation history for these capsules (withdrawn from the ATR in March 2002) is illustrated in Figure 3 of Reference 1. These capsules achieved a LHGR of about 10.7 kW/ft (the highest of any ATR test capsule) at the beginning of Phase II of the irradiation. The pellet, fuel pin, and capsule behaviors at the fuel pellet midplane during the as-run irradiation are predicted by application of the CARTS code.

CARTS calculations for Capsules 4 and 13 were run in advance of the current PIE, each based upon the MCNP-calculated burnup accumulations and corresponding cycle-average LHGRs experienced during the ATR irradiation.

The calculations predict the conditions at the pellet midplane as a function of increasing burnup, and do not include representation of end-effects such as hourglassing. Each capsule surrounds a fuel pin containing 15 MOX pellets. Each pellet has unique dimensions within the specified fabrication tolerances, so that a spectrum of initial pellet-to-clad gaps exists within each fuel pin. In the following discussions, results are reported for the minimum, mean, and maximum initial gap widths as defined by the measured fuel pin inner diameter and the tolerance range for pellet outer diameter.

The CARTS results provide a predicted range for the postirradiation gaps as determined by the initial pellet-clad and clad-capsule gap widths. The fuel thermal conductivity correlation includes a degradation model that causes the fuel conductivity to decrease as burnup increases. This tends to increase the predicted pellet temperatures as irradiation proceeds, in turn causing a greater calculated thermal expansion. The considered densification of two percent complete by 10 GWd/MT burnup is selected to conform to the observations of the 30 GWd/MT PIE.

These CARTS calculations also represent the progressive expansion of the clad as noted in the 30-GWd/MT PIE. This expansion is permanent, persisting after cooling has caused the pellet to shrink away from the clad inner surface. The extent of the outward clad deformation rate is small, about 0.15 mil per 10 GWd/MT burnup.

Figure 3 illustrates the cycle-by-cycle LHGRs as calculated by the MCNP code for Capsule 4, with the corresponding CARTS predictions of pellet mean and centerline temperatures and variations in effective pellet-clad diametral gap. These parameters are plotted against the integrated internal energy release per unit heavy metal mass. The integrated energy release within the capsule is essentially equivalent to the fuel burnup, but includes power sources other than fission such as the small contribution of gamma heating by the ATR core. In the interest of avoiding unnecessary clutter, the LHGR trace does not include spikes to near zero to mark the between-cycle reactor outages.

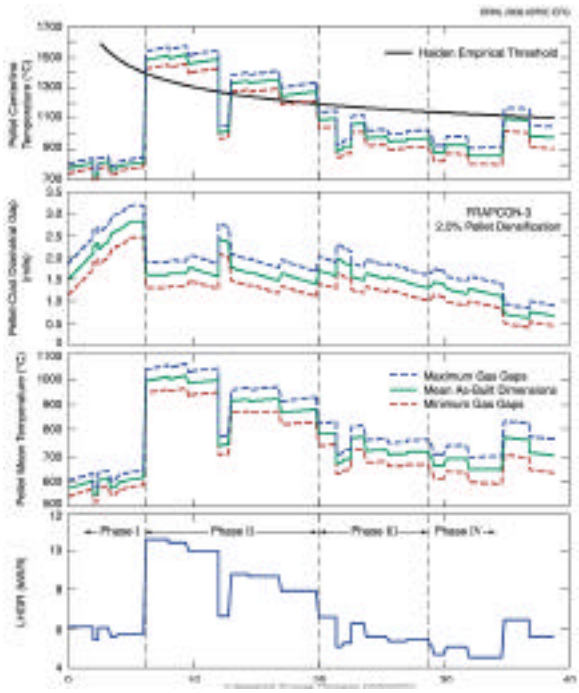

Fig. 3. CARTS predictions for Capsule 4 with representation of outward clad creep. Individual traces show results for maximum, mean, and minimum initial pellet-clad and clad-capsule gap widths.

Three traces are shown in each of the temperature and diametral gap plots, illustrating results as calculated for minimum, mean, and maximum initial pellet-to-clad gap widths. As indicated, the effective diametral gap is predicted to have remained open throughout the irradiation, with a closest approach to closure (for the case of minimum initial gap) of about one-half mil near the end of Phase IV.

With pellet densification of 2.0 percent completed before burnup reaches 10.0 GWd/MT, the pellet diameter initially decreases and remains smaller than its initial value throughout Phase I. This pellet shrinkage combined with outward clad creep causes the predicted pellet-clad diametral gap to almost

double (from 1.49 to 2.83 mils) during this period.

The highest LHGR experienced by Capsule 4 (10.7 kW/ft) was imposed at the beginning of Phase II. As indicated in Figure 3, the accompanying increase in pellet thermal expansion causes the pellet-clad gap to narrow to 1.59 mils. Reduced LHGRs during the subsequent cycles lower the pellet temperature with corresponding reductions in thermal expansion that tend to increase the pellet-clad gap. This trend is countered, however, by monotonically increasing fuel swelling as burnup accumulates. The gap width remains greater than its initial value until near the end of Phase III (integrated energy release of 27.2 GWd/MT).

The increased LHGRs during the last two cycles of Phase IV are due to the shift of the test assembly from the Northwest to the Southwest I-hole in the reflector [in the ATR core the Southwest Lobe normally is higher powered (23 versus 17 MW)]. The higher thermal expansion of the fuel during these cycles reduces the gap width to its smallest value during the irradiation.

As shown in Figure 3, the calculated pellet temperatures increase during periods where the LHGR remains constant during the Phase I and early Phase II irradiation cycles. This reflects the decreases in gap thermal conductance that accompany both an increasing gap width and the increasing inventories of low-conductivity fission gases. The opposite (temperature decrease with shrinking gap under constant LHGR) occurs near the end of Phase IV.

The predicted temperatures are consistently higher for the calculation based on maximum initial pellet–clad gaps. This follows from the lower effective thermal conductance associated with wider gaps. Figure 3 shows that the highest predicted pellet centerline temperature (1581°C) occurs at the end of the second irradiation cycle of Phase II (9.5 GWd/MT). Since this is more than 1000°C below the melting temperature of the MOX fuel, there is no concern for the possibility of fuel melting.

No contact between fuel pin and capsule is predicted at any time during the irradiation.

FISSION GAS RELEASE – APPLICATION OF FRAPCON-3

The Vitanza (or Halden) empirical threshold (Reference 5) for exceeding one percent fission gas release has generally been found applicable to MOX as well as to the UO_2 fuel for which this criterion was originally developed. The upper plot in Figure 3 shows that the fuel centerline temperatures calculated for Capsule 4 exceed the Vitanza threshold during almost all of Phase II, while the integrated energy release was advanced from 6.2 to 19.9 GWd/MT. The single exception is the relatively low-power cycle extending from 12.1 to 12.9 GWd/MT.

The capsules withdrawn at burnups of 21 and 30 GWd/Mt were also predicted to exceed the Vitanza threshold. The fission gas release determined during the PIE (Reference 3) for the 21 GWd/MT capsules (2 and 9) were 1.44 and 1.95 percent, respectively, while the releases for the 30 GWd/MT capsules (3 and 10) were 1.50 and 2.26 percent.

The fission gas release model in FRAPCON-3 has been benchmarked (Reference 4) on gas release data from UO_2 fuel pins. FRAPCON-3 has been modified at ORNL for MOX application with the major changes being (1) the addition of MOX fuel thermal conductivity correlations and (2) user input of the initial plutonium isotopic content. The modified version of FRAPCON-3 has been applied to the capsules withdrawn at burnups of 21, 30, and 40 GWd/MT. The results of these calculations have been superimposed in Figure 4 that is adapted from Reference 6 (a similarly modified version of this figure is also discussed in Reference 1).

The conclusion from Figure 4 is that the "predicted" fission gas release from these MOX test fuel pins is in accordance with the European data cited by Goll (Ref. 6). As shown, the PIE gas release data for the MOX test fuel pins falls below the European trend for similar LHGRs. The difference at least partially derives in that the UO_2 employed in the test fuel was precipitated via the ADU process whereas the European data in Figure 4 uses UO_2 from the AUC process. Historically, MOX fuel using ADU

derived UO_2 has a lower fission gas release rate than MOX fuel with AUC derived UO_2.

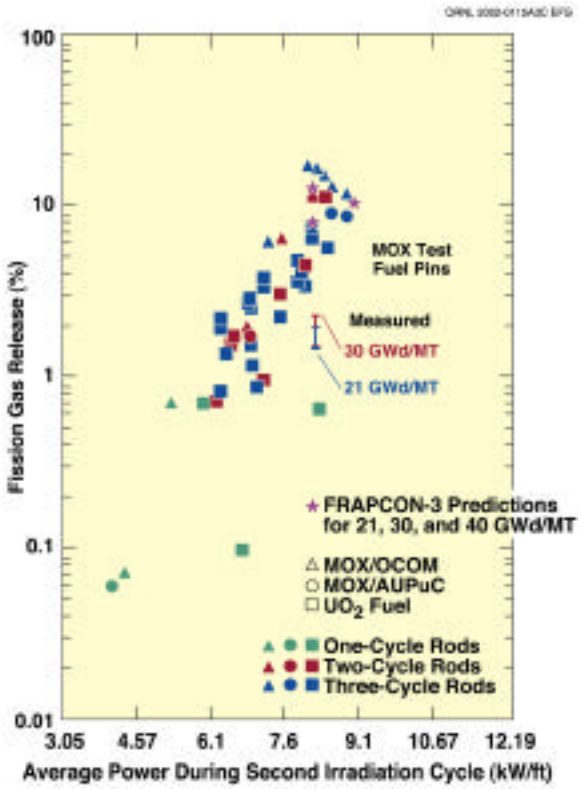

Fig. 4. The MOX test fuel pins exhibit gas release fractions in accordance with linear heat generation rate experience. (Adapted from W. Goll et al., Nuclear Technology, 102, 1993, p. 29.)

CLAD CREEP AND RIDGING

CARTS analyses, which are appropriate for the pellet midplane, predict no hard contact between the pellet and clad through an irradiation of 50 GWd/MT burnup. However, PIE profilometry measurements (Reference 3) of the irradiated MOX fuel pin outer diameter indicate conclusive clad creep outward (as opposed to inward creep in commercial LWR experience) and clad primary “ridging” corresponding to the pellet-to-pellet interfaces. The ridging implies hard pellet-to-clad contact at the interfaces.

Cladding ridges are common in commercial reactor fuel and are the result of (1) differential thermal expansion in the axial direction that causes the fuel pellets to warp into hourglass shapes and (2) high external coolant pressures that cause the cladding to creep inward into contact with the pellets. Commercial fuel is designed with relatively large initial (cold) pellet/cladding gap widths, and localized contact at axial locations near the pellet-to-pellet interfaces does not usually occur until the second fuel cycle.

The unique design characteristics of the MOX test capsules result in a somewhat different sequence of events. Although the PIE measurements show that the test cladding is creeping slowly outward, hourglass-enhanced thermal expansion of the MOX pellets causes localized pellet/cladding contact to occur during initial heatup (at zero burnup) because the test fuel is designed with very small initial gap widths and experiences large linear heat generation rates.

To quantify the amount of cladding ridging expected for the MOX test capsules, the ABAQUS finite element code (Reference 7) has been used to perform several three-dimensional coupled thermal/mechanical analyses. These represent a symmetrical portion of a MOX pellet wedge-shaped fragment (including dish and chamfer, see inset in Figure 5) and adjacent portions of the Zircaloy-4 cladding and stainless steel capsule walls. The thermal portion of ABAQUS predicts the pellet, cladding, and capsule temperatures, while the mechanical models are used to calculate (1) the thermal expansion and associated displacement of the solid structures and (2) the stresses generated by possible contact between the surfaces of the structures.

For conditions representing the initial heatup at 9.1 kW/ft and zero burnup, the closure of the narrow pellet/cladding gap predicted by ABAQUS is shown in Figure 5 as a function of axial position. The outer surface of the MOX pellet expands radially from its initial (cold) position, but no cladding contact is predicted near the pellet midplane (left side of Figure 5). Hourglass-enhanced thermal expansion does cause contact to be predicted for axial positions greater than about 0.10 in. from the pellet midplane, with forced displacement of the cladding in the radial direction reaching a

maximum near the pellet-to-pellet interface (right side of Figure 5). This predicted cladding displacement, however, is not sufficient to cause the outer surface of the cladding to contact the inner surface of the capsule. The cladding stresses predicted by ABAQUS near the location of maximum displacement exceed the Zircaloy-4 yield strength, and some of the cladding displacement shown in Figure 5 will therefore remain as a permanent plastic deformation.

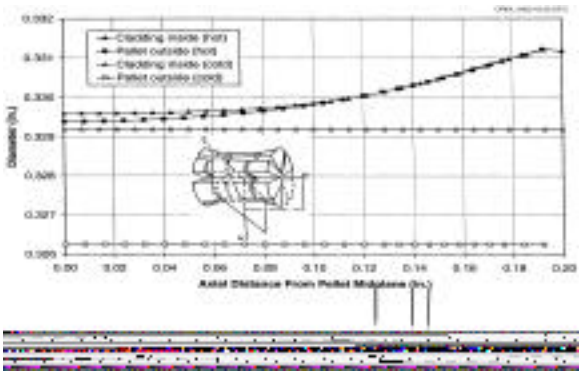

Fig. 5. Predicted pellet/cladding gap diameters at initial (cold) and hot conditions.

SUMMARY

The test MOX fuel, prepared from weapons-derived plutonium, exhibits normal fuel swelling, densification and fission gas release characteristics. The clad and fuel behavior has been as expected from the literature and is well predicted by available computer codes (i.e. CARTS and FRAPCON-3).

The MOX irradiation experimental operating envelope (LHGRs and fuel temperatures) is prototypic of commercial light water reactors with fuel of similar dimensions; however, the test fuel has been irradiated under conditions more severe than will be encountered during the fissile material disposition mission.

There is conclusive evidence of outward clad creep (as opposed to inward creep in commercial LWR experience) and there is clad "ridging" at locations overlying the pellet-to-pellet interfaces. The "ridging" implies hard pellet-to-clad contact at the pellet ends. Three-dimensional thermal/mechanical analyses of the fuel, clad, and capsule wall indicate that the clad creep and "ridging' are primarily due to the effects of pellet "hourglassing."

Fuel performance to date has been excellent. When available, data from future PIEs (combined with the data from the previous PIEs) will be employed to continue the assessment of the MOX fuel behavior in the ATR irradiation.

REFERENCES

1. S. A. Hodge, "Test Irradiation of Mixed-Oxide Fuel Prepared with Weapons-Derived Plutonium," to be presented at the ANS Fifth Topical Meeting on Spent Nuclear Fuel and Fissile Materials Management, Charleston, SC, Sept. 17-20,2002.

2. C. L. Painter, et al., "Fuel Performance Annual Report for 1991," NUREG/CR-3950, vol.9, August 1994.

3. R. N. Morris, et al., "Post Irradiation Examinations of FMDP ATR MOX Fuel," to be presented at the ANS Fifth Topical Meeting on Spent Nuclear Fuel and Fissile Materials Management, Charleston, SC, Sept. 17-20,2002.

4. G. A. Berna, et al., "FRAPCON-3: A Computer Code for the Calculation of Steady-State Thermal-Mechanical Behavior of Oxide Fuel Rods for High Burnup," NUREG/CR-6534, December 1997.

5. C. Vitanza, E. Kolstad, and U. Graziani, "Fission Gas Release From UO_2 Pellet Fuel at High Burnup," ANS Topical Meeting on Light Water Reactor Fuel Performance, Portland, Oregon, 29 April – 3 May, 1979.

6. W. Goll, et al., *Irradiation Behavior of UO_2/PuO_2 Fuel in Light Water Reactors*, **Nuclear Technology**, 102, April 1993, p. 29.

7. ABAQUS/Standard User's Manual Version 5.8, Hibbit, Karlsson and Sorensen, Inc., Pawtucket, Rhode Island, 1998.